Journal of Polymer Science and Engineering (2023) Volume 6 Issue 1
doi: 10.24294/jpse.v6i1.2479

ORIGINAL RESEARCH ARTICLE

Natural convection of hybrid nanofluid with magnetic and thermal effects over an inclined needle

Gundada Raju Rajamani[1], Selvaraj Priya[1], Bhose Ganga[2], Abdul Kaffoor Abdul Hakeem[1,*], Marimuthu Kayalvizhi[3], Pachiyappan Ragupathi[1,*]

[1] *Department of Mathematics, Sri Ramakrishna Mission Vidyalaya College of Arts and Science, Coimbatore 641020, India*
[2] *Department of Mathematics, Providence College for Women, Coonoor 643104, India*
[3] *Department of Mathematics, Government Polytechnic, Daman 396210, India*

*** Corresponding authors:** Abdul Kaffoor Abdul Hakeem, drabdulmaths@gmail.com; P. Pachiyappan Ragupathi, ragupathiprs@gmail.com

ABSTRACT

Hybrid nanofluids have several potential applications in various industries, including electronics cooling, automotive cooling systems, aerospace engineering, and biomedical applications. The primary goal of the study is to provide more information about the characteristics of a steady and incompressible stream of a hybrid nanofluid flowing over a thin, inclined needle. This fluid consists of two types of nanoparticles: non-magnetic nanoparticles (aluminium oxide) and magnetic nanoparticles (ferrous oxide). The base fluid for this nanofluid is a mixture of water and ethylene glycol in a 50:50 ratio. The effects of inclined magnetic fields and joule heating on the hybrid nanofluid flow are considered. The Runge-Kutta fourth-order method is used to numerically solve the partial differential equations and governing equations, which are then converted into ordinary differential equations using similarity transformations. Natural convection refers to the fluid flow that arises due to buoyancy forces caused by temperature differences in a fluid. In the context of an inclined needle, the shape and orientation of the needle have significantly affected the flow patterns and heat transfer characteristics of the nanofluid. These analyses protest that raising the magnetic parameter results in an increase in the hybrid nanofluid thermal profile under slip circumstances. Utilizing the potential of hybrid nanofluids in a variety of technical applications, such as energy systems, biomedicine, and thermal management, requires an understanding of and ability to manipulate these effects.

Keywords: heat transfer; magnetohydrodynamics (MHD); Joule heating; velocity slip; thermal slip

ARTICLE INFO

Received: 21 July 2023
Accepted: 5 September 2023
Available online: 18 October 2023

1. Introduction

Joule heating refers to the process of heat generation that occurs when an electric current passes through a conductor, such as a metal or a fluid. In this research analysis, a fluid flows over a stretching surface with a certain permeability[1]. This study would be used to understand the temperature and concentration distribution, as well as the flow pattern in the fluid[2]. These studies help researchers understand the heat transfer behavior and optimize the design of systems where these effects are significant, such as in energy conversion devices, combustion processes, and thermal management systems[3,4]. Nanofluids are colloidal suspensions with nanoparticles dispersed in base fluids like water, oil, or ethylene glycol. Joule heating is a method for synthesizing nanoparticles in nanofluids by applying high electric current to a precursor solution, facilitating nucleation and growth, and enabling controlled synthesis. This research's improved thermal properties make

them promising candidates for enhancing heat transfer efficiency and improving the overall performance of thermal systems[4]. This research analysis identifies the most influential parameters and natural convective flow, and it's their impact on the system's behavior. This can help optimize the system design or suggest areas for further research[5–8]. This research analysis shows that nanofluid properties impact natural convection in enclosures, with increased thermal conductivity enhancing heat transfer rates. Understanding and optimizing these effects is crucial for efficient use in various heat transfer applications[9–11]. Recent research in the field of hybrid nanofluids is ongoing, and new applications continue to emerge as scientists explore their unique properties and potential in various fields. This study would analyze and interpret the numerical results obtained from the solution. This may involve visualizing the flow patterns, temperature distribution, and other relevant quantities. Compare the results with experimental data or analytical solutions, if available[12]. This study would analyze numerical simulations and analytical solutions that can reveal the impact of SWCNT and MWCNT concentration, magnetic field strength, and other parameters on nanofluid flow patterns, heat transfer, and particle distribution. This is valuable for advanced cooling systems and heat exchangers[13]. This research analyzes Lorentz force and viscous dissipation effects to predict the behavior of a propylene glycol-water mixture containing paraffin wax and sand nanoparticles. This knowledge optimizes system design, controls fluid flow, and enhances heat transfer and transport efficiency[14]. Magnetic fields play a crucial role in various scientific and engineering applications. They have been extensively studied and applied in fields such as materials science, electronics, and medicine. While inclined magnetic fields have not been extensively studied in combination with hybrid nanofluids, the field of magneto rheology is closely related. Magnetorheological fluids (MRFs) are smart fluids that can change rheological properties rapidly due to a magnetic field. These fluids consist of magnetic particles suspended in a carrier fluid, allowing control over flow behavior and viscosity by varying the field strength and orientation. These are just a few examples of how magnetic fields and different geometrical shapes intersect to create various practical applications across multiple industries. The specific geometries are often designed and optimized to achieve the desired performance characteristics for each application[15–23]. Hybrid nanofluids study slip effects through experimental and computational investigations. Computational fluid dynamics (CFD) simulations model fluid flow and heat transfer, while experimental techniques like atomic force microscopy and nanoscale thermometry measure slip effects near solid surfaces. Understanding slip effects in hybrid nanofluids is essential for optimizing their heat transfer performance and designing efficient thermal systems with potential applications in various engineering fields. Some of the following researchers continue to explore this area to harness the full potential of hybrid nanofluids for practical applications[24–26]. Analyzing the Joule heating effect on thin needles in MHD Sakiadis flow using fluid mechanics, electromagnetics, and heat transfer theories[27]. Researchers analyzed MHD boundary layer flows with variable temperature in applications like plasma dynamics, aerospace engineering, and geophysics, enhancing heat transfer, thermal system design, and flow prediction[28]. The study investigated nanofluid flow, heat transfer, and melting behavior in MHD and porous media, impacting engineering and industrial applications like cooling systems, energy conversion, and material processing[29].

The paper aims to study how slip flow conditions around an inclined needle are affected by the presence of an inclined magnetic field and joule heating. The interactions of these factors could lead to changes in flow patterns, temperature distribution, and other fluid dynamic behaviors. One of the primary motivations for using nanofluids is their potential for enhancing thermal conductivity. Research findings might quantify the degree of enhancement achieved due to the inclusion of nanoparticles and the subsequent impact on heat transfer efficiency. Thermal convection refers to the process of heat transmission in fluids due to the combined effect of buoyancy and fluid motion. The application of a Lorentz force can influence fluid stream and heat transmission processes through magnetohydrodynamics (MHD). Joule heating is the heat generated by an electric current in a conducting material, such as an inclined needle, that affects temperature distribution and fluid flow patterns. These effects are of particular interest in various fields such as energy conversion, microfluidics, heat transfer, and magnetic nanoparticle-based therapies, where hybrid nanofluids are used to

enhance heat transfer and control fluid behavior. Researchers continue to investigate and explore the potential applications and benefits of inclined magnetic fields and joule heating effects in such systems.

2. Problem formulation

The acquaintance of contemporary applications is computed underneath:

- The flow is consistent, linear motion, and 2D axisymmetric, which simplifies the flow analysis by reducing the problem to two dimensions.
- The fluid was composed of $H_2O + C_2H_6O_2\ (50-50) + Al_2O_3 + Fe_3O_4$.
- The magnetic field intensity applied normally towards the needle is decided by $B = B(x) = \frac{B_0}{\sqrt{x}}$. $T_\infty\ and\ T_w$ were chosen to represent ambient, surface temperatures.
- The needle passages in the similar or conflicting way as the constant velocity U_w normal with free continual velocity U_∞ and the flow pattern is shown in **Figure 1**.

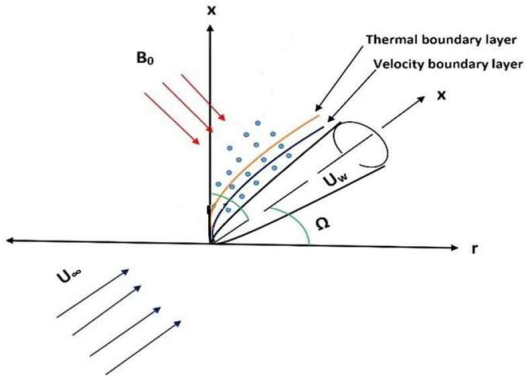

Figure 1. Stream outline of contemporary problem.

These conventions allow for the specification of flow controlling equations as (Sajja et al.[14]):

Continuity equation:

$$r(u)_x + r(v)_r = 0 \tag{1}$$

Momentum equation:

$$uu_x + vu_r = \frac{\mu_{hnf}}{\rho_{hnf}}\left(\frac{1}{r}\right)(ru_r)_r - u\frac{\sigma B^2}{\rho_{hnf}}sin^2\alpha + \frac{g(\rho\beta)_{hnf}(T-T_\infty)}{\rho_{hnf}}\ sin\Omega \tag{2}$$

Energy equation:

$$(\rho C_p)_{hnf}(uT_x + vT_r) = k_{hnf}\left(\frac{1}{r}\right)(rT_r)_r + \sigma B^2u^2 \tag{3}$$

With the boundary conditions, Ganesh et al.[8]:

$$\left.\begin{array}{c} u = U_w + \Gamma_1\left(\frac{\mu_{hnf}}{\rho_{hnf}}\right)\frac{\partial u}{\partial r}\ , v = 0, T = T_w + \Gamma_2\frac{\partial T}{\partial r}atr = R(x) \\ u \to u_\infty, T \to T_\infty\ as \quad r \to \infty \end{array}\right\} \tag{4}$$

The hybrid nanofluid is strategized different volumetric solid fractions (ϕ_1, ϕ_2) such as $Al_2O_3 - (0.5\%)$ and $Fe_3O_4 - (1.5\%)$.

The hybrid nanofluid properties are considered by (Sajja et al.[14]):

$$\rho_{hnf} = \{(1-\phi_2)[(1-\phi_1)\rho_f + \phi_1\rho_{s_1}]\} + \phi_2\rho_{s_2} \tag{5}$$

$$\mu_{hnf} = \frac{\mu_f}{(1-\phi_1)^{2.5}(1-\phi_2)^{2.5}} \tag{6}$$

$$k_{hnf} = \frac{k_{s_2} + 2k_{nf} - 2\phi_2\left(k_{nf} - k_{s_2}\right)}{k_{s_2} + 2k_{nf} + \phi_2\left(k_{nf} - k_{s_2}\right)} \times k_{nf} \tag{7}$$

$$k_{nf} = \frac{k_{s_1} + 2k_f - 2\phi_1\left(k_f - k_{s_1}\right)}{k_{s_1} + 2k_f + \phi_1\left(k_f - k_{s_1}\right)} \times k_f \tag{8}$$

$$\left(\rho C_p\right)_{hnf} = \left\{(1-\phi_2)\left[(1-\phi_1)(\rho C_p)_f + \phi_1(\rho C_p)_{s_1}\right]\right\} + \phi_2(\rho C_p)_{s_2} \tag{9}$$

$$(\rho\beta)_{hnf} = \left\{(1-\phi_2)\left[(1-\phi_1)(\rho\beta)_f + \phi_1(\rho\beta)_{s_1}\right]\right\} + \phi_2(\rho\beta)_{s_2} \tag{10}$$

2.1. Solution to the problem

Along with variables such as, (Sajja et al.[14])

$$\left.\begin{aligned} \eta = \frac{Ur^2}{\nu x}, \psi = \nu x f(\eta), u = \frac{1}{r}\left(\frac{\partial\psi}{\partial r}\right) \\ v = -\frac{1}{r}\left(\frac{\partial\psi}{\partial x}\right), T = T_\infty + (T_w - T_\infty)\theta(\eta) \end{aligned}\right\} \tag{11}$$

we can get $R(x) = \left(\frac{\nu dx}{U}\right)^{\frac{1}{2}}$ where $U = U_w + U_\infty \neq 0$ is the governing equations is satisfied by reinforced acceleration and transforms ((2) to (3)) as:

$$\frac{2J_1J_2}{J_4}\left(\eta F''' + F''\right) - \frac{1}{2J_2}MF'sin^2\alpha + \lambda J_5(sin\Omega)\theta = 0 \tag{12}$$

$$\frac{2J_3J_{31}}{J_4}(\eta\theta'' + \theta') + F\theta' = 0 \tag{13}$$

and changes the circumstances in (4) as,

$$\left.\begin{aligned} F'(d) = \frac{\delta}{2} + \frac{2\gamma_1\sqrt{d}}{J_1J_2}, F(d) = d\left(\frac{\delta}{2} + \frac{2\gamma_1\sqrt{d}}{J_1J_2}\right), \theta(\eta) = 1 + \gamma_2\theta'(\eta) \\ F'(\infty) \to \frac{1-\delta}{2}, \theta(\infty) \to 0 \end{aligned}\right\} \tag{14}$$

The hybrid nanofluid properties are considered by (Sajja et al.[14]):

$$J_1 = (1-\phi_1)^{2.5}(1-\phi_2)^{2.5} \tag{15}$$

$$J_2 = \left\{(1-\phi_2)\left[(1-\phi_1) + \phi_1\frac{\rho_{s1}}{\rho_f}\right]\right\} + \phi_2\frac{\rho_{s2}}{\rho_f} \tag{16}$$

$$J_{31} = \frac{k_{s1} + 2k_f - 2\phi_1\left(k_f - k_{s1}\right)}{k_{s1} + 2k_f + \phi_1\left(k_f - k_{s1}\right)} \tag{17}$$

$$J_3 = \frac{k_{s2} + 2J_{31}k_f - 2\phi_2\left(J_{31}k_f - k_{s2}\right)}{k_{s2} + 2J_{31}k_f + \phi_2\left(J_{31}k_f - k_{s2}\right)} \tag{18}$$

$$J_4 = (1-\phi_2)\left[(1-\phi_1) + \phi_1\frac{(\rho C_p)_{s1}}{(\rho C_p)_f}\right] + \phi_2\frac{(\rho C_p)_{s1}}{(\rho C_p)_f} \tag{19}$$

$$J_5 = (1-\phi_2)\left[(1-\phi_1) + \phi_1\frac{(\rho\beta)_{s1}}{(\rho\beta)_f}\right] + \phi_2\frac{(\rho\beta)_{s2}}{(\rho\beta)_f} \tag{20}$$

$$\lambda = \frac{Gr_x}{\mathrm{Re}_x^{\,2}}, Gr_x = \frac{g\beta_f (T_w - T_\infty)L^3}{\nu^2}, \mathrm{Re}_x = \frac{UL}{\nu}, M = \frac{\sigma B_o^2}{\rho U}, \delta = \frac{U_w}{U} = \frac{\text{constant velocity}}{\text{composite velocity}},$$

$$\lambda = \frac{g\beta_f \left(T_w - T_\infty\right)L}{U^2}, \mathrm{Pr} = \frac{\mu c_p}{k}$$

2.2. Nusselt number and skin friction

Another important external of the contemporary examination is the Nusselt number, Skin friction which is prearranged by (Sajja et al.[14]):

$$N_{ux} = \left.\frac{x q_w}{k_f\left((T_w - T_\infty)\right)}\right|_{r=R(x)} \tag{21}$$

$$C_{fx} = \left.\frac{\tau_w}{\frac{1}{2}\rho U^2}\right|_{r=R(x)} \tag{22}$$

where $q_w = -k_{hnf}\frac{\partial T}{\partial r}$(wall heat flux), $\tau_w = \mu_{hn}\ \frac{\partial u}{\partial r}$ (wall shear stress).

The following terms from (21) and (22) are described in non-dimensional form:

$$(Re_x)^{-\frac{1}{2}} N_{ux} = -J_3 J_{31} 2\sqrt{d}\theta'(d) \tag{23}$$

$$(Re_x)^{-\frac{1}{2}} C_{fx} = \frac{8F''(\eta)\sqrt{d}}{J_1} \tag{24}$$

where $Re_x = \frac{UL}{\nu}$ (Reynolds number).

3. Physical explanation

To analyze this research, we need to resolve the governing equivalences for mass, velocity, and thermal conservation. These equations are typically solved using numerical techniques such as Runge-Kutta fourth order. The governing equations for this problem can be expressed in non-dimensional form using suitable dimensionless variables such as Reynolds variables, Eckert numbers, Prandtl quantities, and inclined magnetic. The transmuted nonlinear differential Equations (1)–(3), and moreover, the boundary restriction (12)–(14), are numerically resolved using the bvp4c solver.

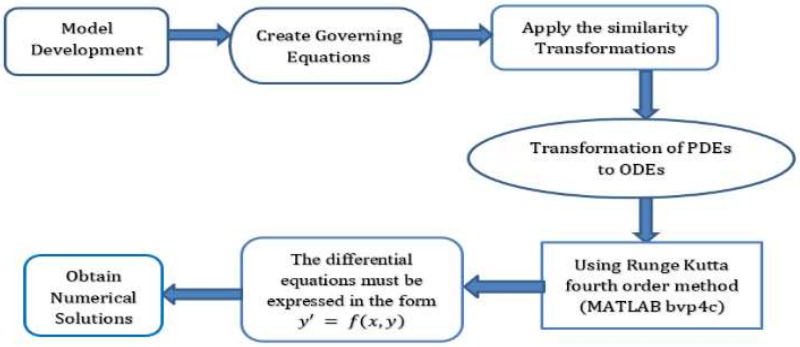

Figure 2. Flow chart for the numerical scheme.

Figure 2 explains the flow chart for the numerical scheme. **Figures 3–12** depict the appearances and structures of various pertinent variables appearing in the problematic profiles of hybrid nanofluid momentum and thermal profile. The values that appear in the problem through computation are fixed as $\phi_1 = 0.005, \phi_2 = 0.015, d = 1, Ec = 0.5, Pr = 29.45,\ M = 3, \delta = 1,\ v_1 = t_1 = 1.5$. **Table 1** demonstrates the importance of

magnetic and nonmagnetic nanoparticle thermophysical properties, as well as hybrid nanofluid thermal properties. **Table 2** displays heat transfer rate and surface drag force values. **Table 3** compares our results to available outcomes in order to validate our problem with other research and discover its remarkable similarity.

Table 1. Thermophysical characteristics attributes of solid volume fractions of nanoparticles and base fluid Ethylene glycol and water (50:50) (T = 300 K) (Iqbal et al.[6] and Ganesh et al.[8]).

-	Specific heat capacity	Density	Thermal conductivity	Thermal expansion coefficient	Prandtl number
Ethylene glycol and water (50:50)	3288	1056	0.425	0.00341	29.45
Aluminium oxide	765	3970	40	0.85	-
Ferrous oxide	670	5180	9.7	1.3	-

Table 2. Difference of M, ϕ_1, ϕ_2, Pr, α on Nu_x and Cf_x.

M	d	ϕ_1	ϕ_2	Pr	α	λ	Ec	Nu_x	Cf_x
1	1	0.005	0.015	29.45	45°	0.5	0.5	1.3417	–90.0234
2								1.2959	–91.8920
3								1.2515	–93.7035
3	1	0.005	0.015	29.45	45°	0.5	0.5	1.2515	–93.7035
	2							1.1519	–52.8420
	3							1.0855	–39.3889
3	1	0.005	0.015	29.45	45°	0.5	0.5	1.2515	–93.7035
		0.010						1.2672	–94.8351
		0.015						1.2829	–96.0030
3	1	0.015	0.005	29.45	45°	0.5	0.5	1.2515	–93.7035
			0.010					1.2666	–94.4641
			0.015					1.2817	–95.2658
3	1	0.005	0.015	1	45°	0.5	0.5	–0.9494	–92.4340
				2				–0.1402	–93.0970
				3				0.2493	–93.3338
3	1	0.005	0.015	29.45	0°	0.5	0.5	1.2515	–93.7035
					45°			1.2515	–93.7035
					90°			1.2515	–93.7035
3	1	0.005	0.015	29.45	45°	0.5	0.5	1.2515	–93.7035
						1.5		1.2515	–93.6478
						2.5		1.2515	–93.5920
3	1	0.005	0.015	29.45	45°	0.5	0.5	1.2515	–93.7035
							1.5	0.9761	–93.6487
							2.5	0.7005	–93.5939

Table 3. Assertion of present rankings when volumetric solid fractions (ϕ_1, ϕ_2) and the velocity ratio parameter δ are zero.

	(Sajja et al.[14])		Present outcomes	
d	$F''(d)$	$-\theta'(d)$	$F''(d)$	$-\theta'(d)$
0.1	1.289074	2.441675	1.287564	2.438536
0.01	8.492173	16.306544	8.490543	16.282928
0.001	62.161171	120.55034	62.148128	120.254769

4. Review and discussion of the results

In regard to physical behaviour and attitude, explanations in **Figures 3–12** have been drawn for EG-Water (50:50) + Al_2O_3 +Fe_3O_4, to demonstrate the impression of numerous parameters on velocity and thermal profile. The Nusselt number and skin friction factors are calculated, and the numerical values with respect to various parameters are displayed in **Table 2**.

4.1. Analysis velocity profile

Figure 3 explains, increase in the magnetic parameter (M) and inclination (Ω) causes stronger magnetic field interaction with current, generating Lorentz force and gravitational force, opposing needle motion. Consequently, the velocity profile of the needle decreases due to the combined effect of these forces.

As a result of the Joule heating effect, increasing the needle size (d) and angle of inclination (Ω) both contribute to an increase in the velocity profile of an inclined needle with the Joule effect. The larger needle size leads to higher resistance and increased heat generation, while a steeper angle of inclination enhances the gravitational force component, resulting in more significant pressure gradients and accelerated flow rates, as explained in **Figure 4**.

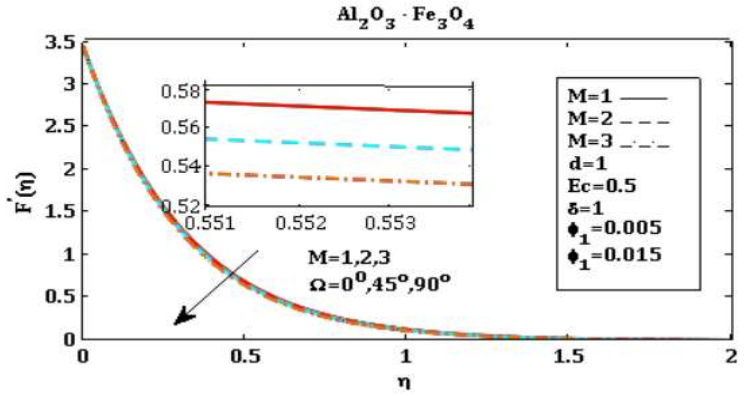

Figure 3. The impacts of $M = 1, 2, 3$ on $F'(\eta)$.

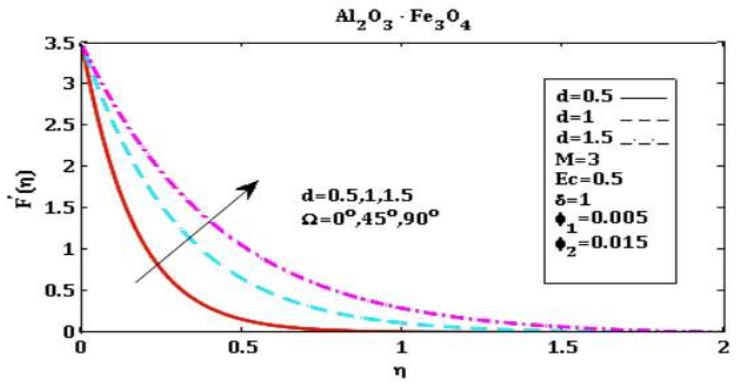

Figure 4. The impacts of $d = 0.5, 1, 1.5$ on $F'(\eta)$.

Figure 5 explains that when the velocity, thermal slip parameter, ($v_1 = t_1$), and angle (Ω) increase, the velocity profile in the inclined needle increases. The fluid flows more rapidly due to higher velocities, improved thermal exchange, and enhanced gravitational force. Consequently, the velocity gradient across the cross-section of the needle increases, leading to an increased velocity profile.

As shown in **Figure 6**, when the ratio of inlet to outlet velocities (δ) increases, the velocity profile becomes flatter and more uniform across the cross-section of the needle. When the angle of inclination (Ω = 0°, 45°, 90°) increases, the velocity profile also increases as the gravitational force enhances the fluid flow.

The combination of these two effects leads to a greater increase in the velocity profile of the inclined needle with the joule heating effect.

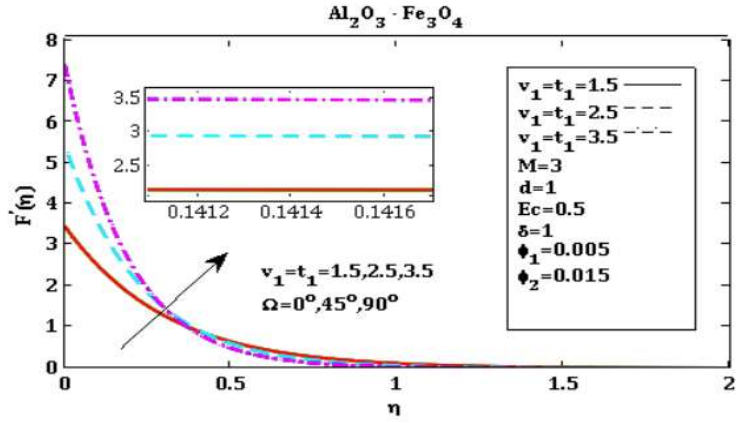

Figure 5. The impacts of $v_1 = t_1 = 1.5, 2.5, 3.5$ on $F'(\eta)$.

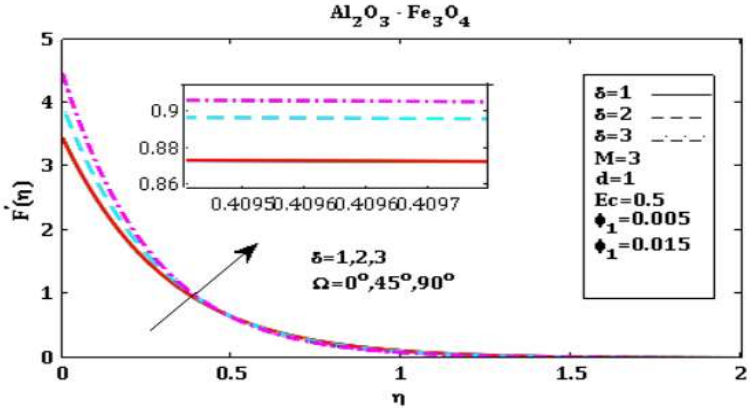

Figure 6. The impacts of $\delta = 1, 2, 3$ on $F'(\eta)$.

Both the mixed convection parameter (λ) and the angle of inclination (Ω) influence on the velocity profile of an inclined needle with the Joule effect are shown in **Figure 7**. Higher values of the mixed convection parameter and steeper inclinations tend to enhance fluid motion and increase velocities. Additionally, the Joule effect, by introducing temperature gradients and associated buoyancy forces, contributes to the amplified velocity profile as shown in **Figure 7**.

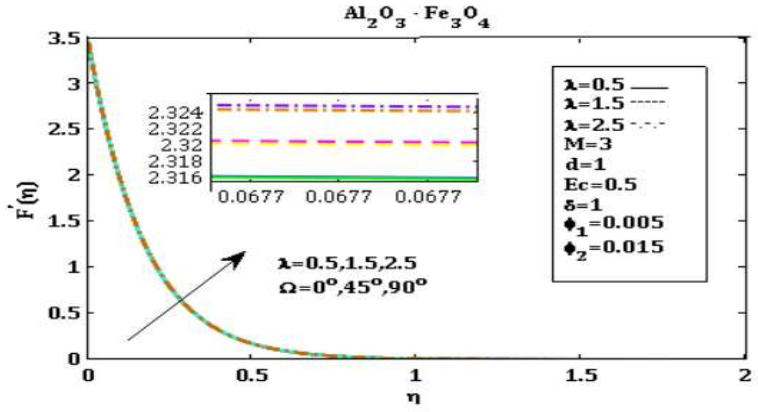

Figure 7. The impacts of $\lambda = 0.5, 1.5, 2.5$ on $F'(\eta)$.

4.2. Analysis thermal profile

Figure 8 explains that as magnetic parameters (M) and angle (Ω) increase, current flow and resistance increase within the conductor, causing higher joule heating and an inclined needle temperature rise. The temperature profile increases because more heat is generated due to the increased Joule effect caused by the stronger magnetic field and steeper inclined needle.

Considering the combinations of needle sizes (d) and angles (Ω), the temperature profile would generally increase with both the needle size and the angle. The highest temperature profile would be observed with the combination of the smallest needle size and the largest angle. This combination results in the highest current density and, consequently, the highest joule heating effect, leading to an increased temperature profile along the inclined needle as exposed in **Figure 9**.

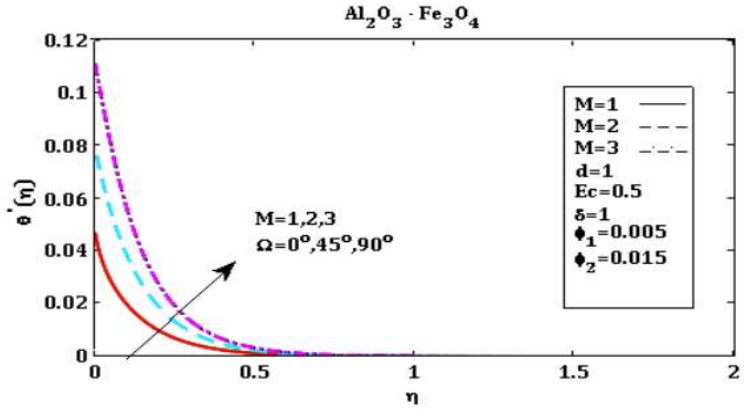

Figure 8. The impact of M = 1, 2, 3 on $\theta'(\eta)$.

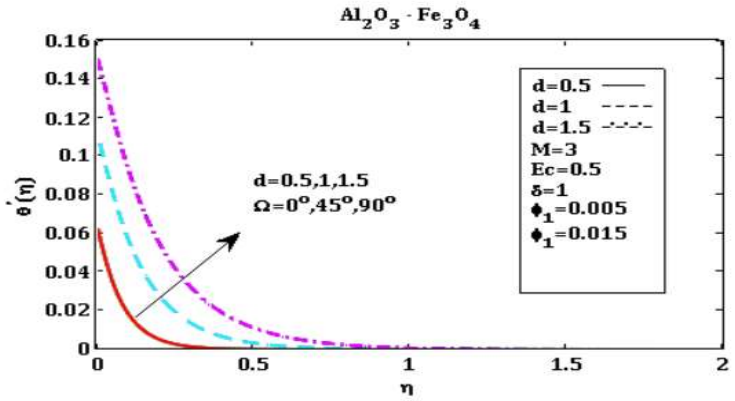

Figure 9. The impact of d = 0.5, 1, 1.5 on $\theta'(\eta)$.

Figure 10 explains that when all these parameters (velocity, thermal slip parameter, and angle) $(v_1 = t_1)$, and (Ω) increase, the temperature profile along the inclined needle will generally increase. These factors enhance the rate of heat transfer and the available surface area for energy exchange, leading to a higher temperature distribution along the surface of the needle.

The increased velocity ratio parameter (δ) and angle (Ω) contribute to improved convective heat transfer, effectively reducing the temperature gradients along the inclined needle's length. Increasing these parameters enhances the convective heat transfer, resulting in a higher temperature profile along the length of the inclined needle with the Joule heating effect, as explained in **Figure 11**.

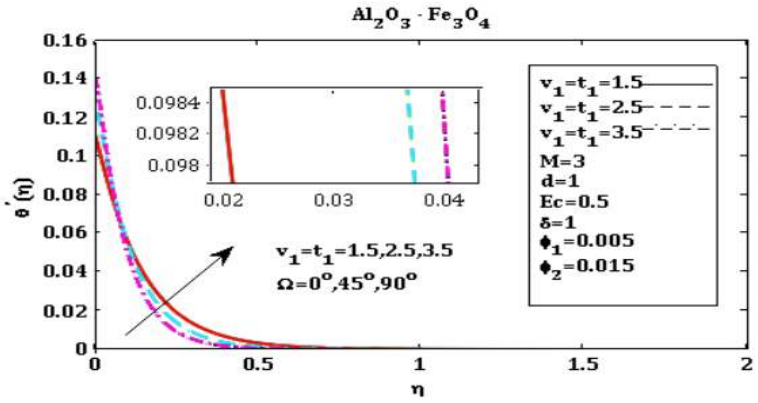

Figure 10. The impact of $v_1 = t_1 = 1.5, 2.5, 3.5$ on $\theta'(\eta)$.

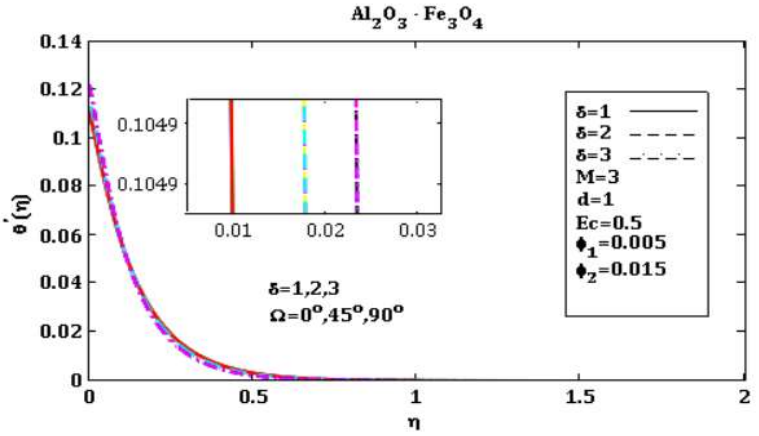

Figure 11. The impacts of $\delta = 1, 2, 3$ on $\theta'(\eta)$.

Figure 12 explains that an increase in the Eckert number (Ec) and angle of inclination (Ω) leads to a higher temperature profile in the inclined needle with the Joule effect. A higher Eckert number means more kinetic energy relative to enthalpy, resulting in a steeper temperature rise near the needle's surface. Meanwhile, a larger angle of inclination provides a larger surface area for heat transfer, leading to a faster temperature rise along the needle's surface.

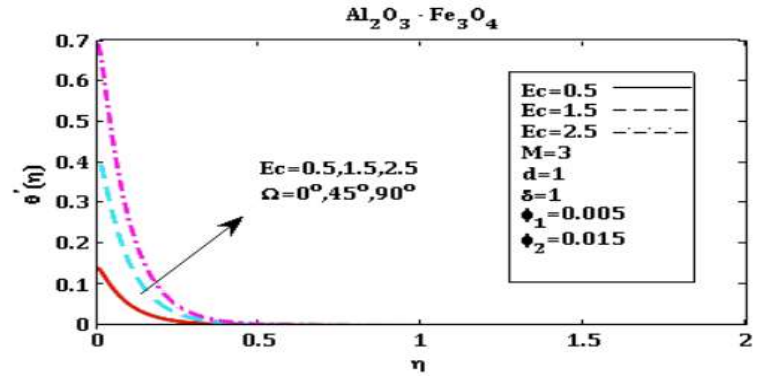

Figure 12. The impacts of $Ec = 0.5, 1.5, 2.5$ on $\theta'(\eta)$.

5. Conclusion

The article investigated the specific problem of fluid flow around a thin needle that is in motion, considering laminar flow, incompressible fluid behavior, and slip effects related to both velocity and temperature. A summary of the analysis is presented in the sections that follows:

- This research optimizes the system for specific applications. This could involve finding the optimal

nanoparticle concentration, magnetic field strength, and inclination angle to achieve the desired heat transfer rates.

- The presence of nanoparticles in the fluid, along with the application of a magnetic field, leads to enhanced heat transfer rates. This effect is particularly pronounced when considering an inclined needle geometry.
- The convective heat transfer coefficient is significantly improved compared to traditional fluids, making hybrid nanofluids promising for various heat transfer applications.
- These results demonstrate that the velocity and thermal profiles of an inclined needle with joule heating effect are influenced by various physical parameters, such as magnetic field strength, angle of inclination, slip conditions, and needle size.
- This has important implications for designing and optimizing nanofluid-based drug delivery systems that can target specific tissues or organs in a controlled manner.

Author contributions

Conceptualization, GRR, SP, BG, AKAH, MK and PR; methodology, GRR, SP, AKAH and PR; software, SP, BG and MK; validation, AKAH, BG and PR; formal analysis, AKAH and PR; investigation, AKAH and PR; resources, GRR and SP; data curation, SP and MK; writing—original draft preparation, SP; writing—review and editing, SP and PR ; visualization, SP and BG; supervision, AKAH and PR; project administration, AKAH; funding acquisition, BG. All authors have read and agreed to the published version of the manuscript.

Conflict of interest

The authors declare no conflict of interest.

Abbreviations

Nomenclature

B =	magnetic field intensity, $kgs^{-2}a^{-1}$
C_f =	skin friction coefficient
C_p =	specific heat, $jkg^{-1}k^{-1}$
K =	thermal conductivity, $wm^{-1}k^{-1}$
M =	magnetic parameter
Nu_x =	local Nusselt number
Pr =	prandtl number
q_w =	surface heat flux, wm^{-2}
Re =	local Reynolds number
Ec =	Eckert number
Gr_x =	Grashof number
$R(x)$ =	equivalence of the surface of a thin needle
F =	Dimensionless fluid velocity
T =	temperature of fluid
T_w =	ambient thermal
T_∞ =	surface thermal
U =	reference velocity, ms^{-1}
U_w =	constant velocity
U_∞ =	free stream momentum
u =	momentum factor in the x way
x , r =	cylindrical directs

Greek letters

α =	angle
η =	the magnitude of the needle (η = d)
ϕ_1, ϕ_2 =	nanoparticles of volume fraction
μ =	dynamic viscosity, $kgm^{-1}s^{-1}$
υ =	kinematic viscosity, m^2s^{-1}
σ =	electrical conductivity, sm^{-1}
ρ =	density, kgm^{-3}

θ =	dimensionless fluid temperature
λ =	Mixed convection parameter
δ =	velocity ratio parameter
ψ =	dimensionless stream function
τ_w =	wall shear stress, nm^{-2}
Γ_1 =	velocity slip factor
Γ_2 =	thermal slip factor
γ_1 =	velocity slip coefficient
γ_2 =	thermal slip coefficient

Subscripts

hnf =	hybrid nanofluid
nf =	nanofluid
f =	fluid
s =	solid

References

1. Magyari E, Keller B. Exact solutions for self-similar boundary-layer flows induced by permeable stretching walls. *European Journal of Mechanics-B/Fluids* 2000; 19(1): 109–122. doi: 10.1016/S0997-7546(00)00104-7
2. Ibrahim SM. Unsteady MHD convective heat and mass transfer past an infinite vertical plate embedded in a porous medium with radiation and chemical reaction under the influence of Dufour and Soret effects. *Chemical and Process Engineering Research* 2014; 19: 25–38.
3. Cortell R. Combined effect of viscous dissipation and thermal radiation on fluid flows over a non-linearly stretched permeable wall. *Meccanica* 2012; 47(3): 769–781. doi: 10.1007/s11012-011-9488-z
4. Oke AS, Mutuku WN. Significance of Coriolis force on Eyring-Powell flow over a rotating non-uniform surface. *Applications and Applied Mathematics: An International Journal* 2021; 16(1): 36.
5. Choi SUS, Eastman JA. Enhancing thermal conductivity of fluids with nanoparticles. In: Proceedings of the ASME International Mechanical Engineering Congress & Exposition; 12–17 November 1995; San Francisco, USA.
6. Iqbal Z, Yashodha S, Hakeem AK, et al. Energy transport analysis in natural convective flow of water: Ethylene glycol (50:50)-based nanofluid around a spinning down-pointing vertical cone. *Frontiers in Materials* 2022; 9: 1037201. doi: 10.3389/fmats.1037201
7. Sankar M, Park J, Do Y. Natural convection in a vertical annuli with discrete heat sources. *Numerical Heat Transfer, Part A: Applications* 2011; 59(8): 594–615. doi: 10.1080/10407782.2011.561110
8. Ganesh NV, Al-Mdallal QM, Reena K, Aman S. Blasius and Sakiadis slip flow of H_2O–$C_2H_6O_2$ (50:50) based nanoliquid with different geometry of boehmite alumina nanoparticles. *Case Studies in Thermal Engineering* 2019; 16: 100546. doi: 10.1016/j.csite.2019.100546
9. Abu-Nada E, Masoud Z, Oztop HF, Campo A. Effect of nanofluid variable properties on natural convection in enclosures. *International Journal of Thermal Sciences* 2010; 49(3): 479–491. doi: 10.1016/j.ijthermalsci.2009.09.002
10. Reddy NK, Sankar M. Buoyant convective transport of nanofluids in a non-uniformly heated annulus. *Journal of Physics: Conference Series* 2020; 1597(1): 012055. doi: 10.1088/1742-6596/1597/1/012055
11. Sankar M, Kiran S, Ramesh GK, Makinde OD. Natural convection in a non-uniformly heated vertical annular cavity. *Defect and Diffusion Forum* 2017; 377: 189–199. doi: 10.4028/www.scientific.net/DDF.377.189
12. Shoaib M, Raja MA, Sabir MT, et al. Numerical investigation for rotating flow of MHD hybrid nanofluid with thermal radiation over a stretching sheet. *Scientific Reports* 2020; 10(1): 18533. doi: 10.1038/s41598-020-75254-8
13. Al-Hanaya AM, Sajid F, Abbas N, Nadeem S. Effect of SWCNT and MWCNT on the flow of micropolar hybrid nanofluid over a curved stretching surface with induced magnetic field. *Scientific Reports* 2020; 10(1): 8488. doi: 10.1038/s41598-020-65278-5
14. Sajja VS, Gadamsetty R, Muthu P, et al. Significance of Lorentz force and viscous dissipation on the dynamics of propylene glycol: Water subject to Joule heating conveying paraffin wax and sand nanoparticles over an object with a variable thickness. *Arabian Journal for Science and Engineering* 2022; 47(12): 15505–15518. doi: 10.1007/s13369-022-06658-z
15. Guedri K, Raizah Z, Eldin ET, et al. Thermal mechanism in magneto radiated $[(Al_2O_3 - Fe_3O_4)/\text{blood}]_{\text{hnf}}$ over a 3D surface: Applications in biomedical engineering. *Frontiers in Chemistry* 2022; 10: 960349. doi: 10.3389/fchem.2022.960349
16. Al-Mdallal QM, Indumathi N, Ganga B, Hakeem AA. Marangoni radiative effects of hybrid-nanofluids flow past a permeable surface with inclined magnetic field. *Case Studies in Thermal Engineering* 2020; 17: 100571. doi: 10.1016/j.csite.2019.100571
17. Sankar M, Park Y, Lopez JM, Do Y. Double-diffusive convection from a discrete heat and solute source in a vertical porous annulus. *Transport in Porous Media* 2012; 91: 753–775. doi: 10.1007/s11242-011-9871-1

18. RamReddy C, Saran HL. Linear temporal stability analysis of dual solutions for a Ti-alloy nanofluid with inclined MHD and Joule effects: Flow separation. *Journal of Nanofluids* 2022; 11(5): 782–794. doi: 10.1166/jon.2022.1870
19. Ramzan M, Dawar A, Saeed A, et al. Heat transfer analysis of the mixed convective flow of magnetohydrodynamic hybrid nanofluid past a stretching sheet with velocity and thermal slip conditions. *PLOS One* 2021; 16(12): 0260854. doi: 10.1371/journal.pone.0260854
20. Swamy HAK, Sankar M, Reddy NK. Analysis of entropy generation and energy transport of Cu-water nanoliquid in a tilted vertical porous annulus. *International Journal of Applied and Computational Mathematics* 2022; 8: 10. doi: 10.1007/s40819-021-01207-y
21. Govindaraju M, Saranya S, Hakeem AA, et al. Analysis of slip MHD nanofluid flow on entropy generation in a stretching sheet. *Procedia Engineering* 2015; 127: 501–507. doi: 10.1016/j.proeng.2015.11.405
22. Khashi'ie NS, Arifin NM, Pop I. Magnetohydrodynamics (MHD) boundary layer flow of hybrid nanofluid over a moving plate with Joule heating. *Alexandria Engineering Journal* 2022; 61(3): 1938–1945. doi: 10.1016/j.aej.2021.07.032
23. Ullah H, Fiza M, Khan K, et al. Effect of Joule heating and thermal radiation of MHD boundary layer Oldroyd-B nanofluid flow with heat transfer over a porous stretching sheet by finite element method. *Journal of Nanomaterials* 2022; 2022: 7373631. doi: 10.1155/2022/7373631
24. Sejunti MI, Khaleque TS. Effects of velocity and thermal slip conditions with radiation on heat transfer flow of ferrofluids. *Journal of Applied Mathematics and Physics* 2019; 7(6): 1369–1387. doi: 10.4236/jamp.2019.76092
25. Sen SSS, Das M, Nayak MK, Makinde OD. Natural convection and heat transfer of micropolar hybrid nanofluid over horizontal, inclined and vertical thin needle with power-law varying boundary heating conditions. *Physica Scripta* 2023; 98(1): 015206. doi: 10.1088/1402-4896/aca3d7
26. Hussain A, Akkurt N, Rehman A, et al. Transportation of thermal and velocity slip factors on three-dimensional dual phase nanomaterials liquid flow towards an exponentially stretchable surface. *Scientific Reports* 2022; 12: 18595. doi: 10.1038/s41598-022-21966-y
27. Sulochana C, Ashwinkumar GP, Sandeep N. Joule heating effect on a continuously moving thin needle in MHD Sakiadis flow with thermophoresis and Brownian moment. *The European Physical Journal Plus* 2017; 132: 387. doi: 10.1140/epjp/i2017-11633-3
28. Naseem T, Fatima U, Munir M, et al. Joule heating and viscous dissipation effects in hydromagnetized boundary layer flow with variable temperature. *Case Studies in Thermal Engineering* 2022; 35: 102083. doi: 10.1016/j.csite.2022.102083
29. Tarakaramu N, Sivakumar N, Satya Narayana PV, Sivajothi R. Viscous dissipation and Joule heating effects on 3D magnetohydrodynamics flow of Williamson nanofluid in a porous medium over a stretching surface with melting condition. *ASME Open Journal of Engineering* 2022; 1: 011033. doi: 10.1115/1.4055183